Received: 6 January 2017 | Accepted: 5 May 2017
DOI: 10.1002/jcp.25991

ORIGINAL RESEARCH ARTICLE

WILEY Journal of Cellular Physiology

The influence of rAAV2-mediated SOX2 delivery into neonatal and adult human RPE cells; a comparative study

Razie Ezati[1] | Azadeh Etemadzadeh[1] | Zahra-Soheila Soheili[1] | Shahram Samiei[2] | Ehsan Ranaei Pirmardan[3] | Malihe Davari[1] | Hoda Shams Najafabadi[1]

[1] Institute of Medical Biotechnology, National Institute of Genetic Engineering and Biotechnology, Tehran, Iran

[2] Blood Transfusion Research Center, High Institute for Research and Education in Transfusion Medicine, Tehran, Iran

[3] Faculty of Basic sciences, Tarbiat Modarres University, Tehran, Iran

Correspondence
Zahra-Soheila Soheili, Ministry of Science, Research and Technology, National Institute of Genetic Engineering and Biotechnology, P.O. Box: 14965/161, Pajoohesh Boulevard, 17th Kilometers, Tehran-Karaj Highway, Tehran, Iran.
Email: soheili@nigeb.ac.ir; zahrasoheila@yahoo.com

Cell replacement is a promising therapy for degenerative diseases like age-related macular degeneration (AMD). Since the human retina lacks regeneration capacity, much attention has been directed toward persuading for cells that can differentiate into retinal neurons. In this report, we have investigated reprogramming of the human RPE cells and concerned the effect of donor age on the cellular fate as a critical determinant in reprogramming competence. We evaluated the effect of SOX2 over-expression in human neonatal and adult RPE cells in cultures. The coding region of human SOX2 gene was cloned into adeno-associated virus (AAV2) and primary culture of human neonatal/adult RPE cells were infected by recombinant virus. De-differentiation of RPE to neural/retinal progenitor cells was investigated by quantitative real-time PCR and ICC for neural/retinal progenitor cells' markers. Gene expression analysis showed 80-fold and 12-fold over-expression for SOX2 gene in infected neonatal and adult hRPE cells, respectively. The fold of increase for Nestin in neonatal and adult hRPE cells was 3.8-fold and 2.5-fold, respectively. PAX6 expression was increased threefold and 2.5-fold in neonatal/adult treated cultures. Howbeit, we could not detect rhodopsin, and CHX10 expression in neonatal hRPE cultures and expression of rhodopsin in adult hRPE cells. Results showed SOX2 induced human neonatal/adult RPE cells to de-differentiate toward retinal progenitor cells. However, the increased number of PAX6, CHX10, Thy1, and rhodopsin positive cells in adult hRPE treated cultures clearly indicated the considerable generation of neuro-retinal terminally differentiated cells.

KEYWORDS
neural progenitor cells, retinal pigmented epithelial cells (RPE), retinal progenitor cells (RPC), SOX2 gene

1 | INTRODUCTION

Retina, the innermost layer of the eye, is originated from embryonic optic cup and as the optic cup is made up of two main layers including inner and outer layers. The inner layer called neural retina that consists of neurons and photoreceptors and the outer layer is retinal pigmented epithelium (RPE). Neural retina is made up of seven main classes of retinal cell types including rod, cone, bipolar, horizontal, amacrine, ganglion, and müller glial cells which are produced from a pool of multipotent retinal progenitor cells (RPC) (Cepko, 2014). Neurodegenerative diseases in retina such as age-related macular degeneration

Razie Ezati and Azadeh Etemadzadeh contributed equally to this study.

(AMD) and retinitis pigmentosa (RP) lead to the loss of these cells and irreversible blindness. Since retinal cells cannot regenerate after getting damaged, finding cells that can differentiate into retinal neurons would have significant impact in treatment of retinal diseases. Since the non-neural RPE and the neural retina developmentally originate from the same structure—the optic vesicle—this common origin may give them the same cellular and molecular characteristic and may help RPE to convert to retinal progenitor/neural cells (John et al., 2013; Wang, Ma, Yan, & Mao, 2010). It has been shown that RPE cells retain cellular plasticity and demonstrate the ability of dedifferentiation, transdifferentiation, or reprogramming (Fuhrmann, Zou, & Levine, 2014; Luz-Madrigal et al., 2014; Yan, Li, & Wang, 2013).

Culturing isolated RPE in defined culture conditions releases their normal quiescence and stimulates self-renewal capability, and reveals multipotency, which designates the RPE stem cell (RPESC) phenotype. RPESCs did not exhibit pluripotency and are not an exemplar neural stem cells, but rather they are a new type of stem cell that is able to produce both CNS and mesoderm-associated lineages, particularly mesenchymal progeny (Salero et al., 2012).

Studies have demonstrated that fetal/adult hRPE both can proliferate in culture and produce a valuable monolayer for studying RPE function and biology (Blenkinsop, Salero, Stern, & Temple, 2013).

However, it has been demonstrated that only a subpopulation of RPE cells in culture can proliferate extensively. These RPESCs can be stimulated in culture to self-renew and produce multipotent proliferating cells (Salero et al., 2012).

Many studies examined the potency of small molecules, FGF-1, FGF2 and EGF, and amniotic fluid in trans-differentiation of RPE toward retinal neurons in xenopus, chick embryo, and human (Davari et al., 2013; Lamba, Karl, & Reh, 2008). In other studies, transcription factors involved in regulation of retina development have been used for the assessment of RPE trans-differentiation. These studies showed neurogenin gene family (NGN1, NGN2, NGN3), PAX6 and SOX2 are able to induce chick RPE toward retinal neurons (Li, Ma, Zhuo, Yan, & Wang, 2010; Ma, Yan, Li, & Wang, 2009; Yan et al., 2010). Recent studies have shown that a single transcription factor, Sox2, is sufficient to convert human fetal RPE cells to functional neurons (Hu, Chen, Teesalu, Ruoslahti, & Clegg, 2014).

Sry-related high mobility group box (SOX) family is highly conserved transcription factors in vertebrates and invertebrates. This family of transcription factors is composed of 20 members that bear high mobility group DNA binding domain (HMG-box) for binding to the DNA sequence. SOX family is divided into eight subfamilies (A–H) based on HMG-box similarity. SOXB1 subfamily has three members (SOX1-SOX2-SOX3) which their function and expression are important in neural progenitor cells' viability and functions. SOXB1 factors show unique expression patterns in developing eye so that SOX1-SOX2-SOX3 initially express in the neural plate and invaginating optic vesicle. During the formation of optic cup, SOX1 and SOX3 are downregulated, while SOX2 expression maintained and confined to neural retinal cells (Taranova et al., 2006). Permanent expression of SOX2 inhibits neuronal differentiation while inhibition of SOX2 signaling leads to the loss of progenitor markers, precocious cell cycle exit, and initiation of neuronal differentiation. So SOX2 maintains neural progenitor identity (Sarkar & Hochedlinger, 2013). SOX2 expression in neural stem cells and progenitors also occurs in neurogenesis of adulthood (Ferri et al., 2004).

Cellular senescence affects the reprogramming efficiency (Banito et al., 2009; Li et al., 2009) The intrinsic properties of the interested somatic cells, also, determine the reprogramming efficiency. Reprogramming efficiency of murine cells has been shown to be affected by donor age (Wang et al., 2011). However, donor age was suggested not to impair the reprogramming efficiency of human cells (Somers et al., 2010).

Although several articles were published in recent years that performed reprogramming of RPE by SOX2, as a necessary reprogramming growth factor (Chen et al., 2010), none of them have investigated reprogramming of human neonatal/adult RPE cells and none of them have compared the effect of age on the reprogramming cell fate.

In the current study, adeno-associated virus (AAV2) harboring human SOX2 gene used to assess the effect of SOX2 over-expression in human neonatal/adult RPE cells in culture and to compare the cell fate of the cultures that were originated from neonatal and adult donors RPE.

The advantages of AAV vector over other vectors, in particular, a relative lack of pathogenicity and long-term maintenance of transgene expression in the eye (Raisler, Deng, Berns, & Hauswirth, 2005), inspired us to use this vector for SOX2 gene over-expression in cultured RPE cells.

2 | METHODS

2.1 | Construction of gene expression cassette

The coding sequence of human SOX2 gene was synthesized and cloned into the PCR 2.1 cloning vector by Eurofin MWG Operon Company (Huntsville, AL). In order to subclone the SOX2 gene into the pAAV-MCS vector (Agilent, Brussels, Belgium), vector digestion by *Bam*HI and *Xho*I restriction enzymes was done and then the resulted gene containing segment was ligated into the *Bam*HI/*Xho*I site of the pAAV-MCS expression vector. In order to determine gene transfection efficiency, the coding sequence of enhanced GFP (eGFP) was digested by *Bgl*II and *Xho*I restriction enzymes and ligated into the *Bgl*II and *Xho*I site of the pAAV-SOX2 vector in downstream of SOX2 gene and the resultant vector designated as pAAV-SOX2-GFP construct. The recombinant construct was confirmed by PCR, restriction digestion, and finally DNA sequencing.

2.2 | Recombinant AAV-2 viral particles propagation

AAV-2 viral particles were produced by calcium-phosphate method for transfection of HEK293T; human embryonic kidney cells. HEK293T cells were plated in 15-cm plates at a density of 80×10^5 cells in 8 ml DMEM (Invitrogen, Brussels, Belgium) supplemented with 10% FBS (Gibco, Melbourne, Australia) 24 hr prior to transfection. Freshly complete culture medium was added to each plate, 1–2 hr before

transfection. The following amount of DNA was used per culture plate: 40 μg pAAV-SOX2-GFP vectors, 15 μg pAAV-RC plasmid encoding replication and capsid genes, and 20 μg pHelper vector. The aforesaid vectors were mixed together in 836 μl H_2O and 125 μl 2M $CaCl_2$. The vector mixture was added to 1,000 μl of 2× HEPES-buffered saline (HBS), under gentle vortexing, and then was finally pipetted into the medium, after 20-min incubation in room temperature. Six hours after transfection, the medium was replaced with fresh medium. Seventy-two hours after transfection, recombinant AAV2s (rAAV2s) were harvested, purified, and concentrated by using HiTrap Heparin HP (GE Healthcare Life Sciences, Boston, MA) and Amicon® Ultra 4 mL Filters (Boston, MA). Briefly, cell culture media was removed and discarded, cells were washed in warm PBS (1×; was prepared by dissolving 8 g NaCl, 0.2 g KCl, 2.68 g Na_2HPO_4-$7H_2O$, and 0.24 g KH_2PO_4 in ddH_2O, thereupon pH was adjusted to 7.4 and total volume was adjusted to 1L) and were gently removed with a cell scraper and centrifuged at 800*g* for 10 min. Cell pellet was re-suspended in lysis buffer (150 mM NaCl, 20 mM Tris pH 8.0 Merck, Darmstadt, Germany) and sodium deoxycholate was added to the cell suspension for a final concentration of 0.5%. Afterward benzonase nuclease (Sigma, Munich, Germany) with a final concentration of 50 U/ml was added and tube incubated at 37°C for 1 hr. Then cellular debris were removed by centrifugation at 12,000*g* for 30 min and supernatant was applied to heparin column which had previously been equilibrated by 10 ml 150 mM NaCl, 20 mM Tris pH 8.0. The lysate was allowed to flow through and column was washed with 20 ml 100 mM NaCl, 20 mM Tris pH 8.0. Washing the column was continued using 5-ml syringes with 1 ml 200 mM NaCl, 20 mM Tris pH 8.0, followed by 1 ml 300 mM NaCl, 20 mM Tris pH 8.0 and the flow-through was discarded. The virus preparations was eluted from the column by applying 1.5 ml 400 mM NaCl, 20 mM Tris pH 8.0, 3 ml 450 mM NaCl, 20 mM Tris pH 8.0, and 1.5 ml 500 mM NaCl, 20 mM Tris pH 8.0. The final flow through liquid was collected in a 15-ml tube. In the final step, concentration of the sample with Amicon Ultra 4 ml filters (UFC810024) was done and the collected viral particles were stored at −80°C until required. All the mentioned procedures were done for the production of AAV2-eGFP virus particles as well.

2.3 | Titration of viral stocks

Flow cytometry was performed to determine infectious virus particles. HEK293T cells were cultured in six-well cell culture plates. After 24 hr, cells were infected by AAV2-SOX2-GFP or AAV2-GFP virus and cell culture media was replaced 8 hr post-infection. AAV2-SOX2-GFP- and AAV2-GFP-infected HEK293T cells were trypsinized 48 hr post-infection. Cell's pellet was re-suspended in an appropriate volume of cold PBS so that the final cell concentration was 5×10^6/ml, then flow cytometry was performed.

Quantitative PCR was done in order to determine genomic particles.

pAAV-MCS plasmid in four different dilutions was used to create genomic DNA (gDNA) standard. Specific primers for CMV promoter (Table 1) were applied in QPCR.

2.4 | Primary culture of RPE cells

Neonatal/adult globes between 24 hr and 48 hr after death of the donors were obtained from the Eye Bank of Iran, which subordinates the rules and regulations of an ethics committee which is under supervision of global requirements. RPE cell culture was carried out under sterile conditions.

Excessive muscles and connective tissue around the eye were trimmed using scissors. An incision was made below cornea and the anterior portion and its contents were lift away. The opened eye was transferred to new plate and neural retina was removed and the remaining part of the eye was rinsed several times with PBS to eliminate remaining neural tissues, blood, and other tissue residuals. Afterward, the RPE layer was amputated from underlying tissue and minced into small sections and then was incubated in 1.1 U/ml of Dispase I solution (Invitrogen) at 37°C for 50 min. Subsequently, the sample was centrifuged at 300*g* and 4°C for 5 min. The resulting cellular pellet was re-suspended in culture medium and was cultured in 25-cm^2 flasks (Nunc, Roskilde, Denmark) which were previously coated with fetal bovine serum (FBS, Gibco) and was incubated in a humidified atmosphere of 5% CO_2 at 37°C.

At the first passage, culture medium was being prepared by a mixture of DMEM and Hams F12 (Invitrogen) supplemented with 20% FBS, streptomycin (220 μg/ml, Fluka, Brussels, Belgium), penicillin (120 μg/ml, Fluka), and amphotericin B (2.5 μg/ml, Gibco). Then successful cultures were maintained in medium supplemented with 10% FBS until the cells reached to 90% confluent. Thereupon cells were sub-cultured and were seeded at a ratio of 3×10^5 cells per 25-cm^2 flask.

All cultures have been assessed and compared in similar densities. Representative pictures have been taken from the beginning of primary cultures until they reached a full confluence.

Near confluent cultures from passages 3–5 were employed in all experiments.

2.5 | Transduction of human neonatal/adult RPE cells

Neonatal/adult human RPE (hRPE) cells were cultured as already noted. Confluent cells were trypsinized and centrifuged in 300 g for 5 min. Cells' pellets were resuspended in DMEM/F12 in the presence of 2% FBS and cell counting was done. RPE cells (10^5) were infected with rAAV2-SOX2-GFP at a multiplicity of infection (MOI) of 10. Twelve hours post-infection, cell culture medium was exchanged with

TABLE 1 Primer list which has been used in quantitative real-time PCR

Primer	Forward	Reverse
PCMV	TGGATAGCGGTTTGACTCAC	ATGGGGCGGAGTTGTTACGA
CHX10	TCGTGATATGCTGCTTGTG	CTGTGGCTTCGTAGATGTC

DMEM/F12 supplemented with 10% FBS. As a control, infection of hRPE cells was done by rAAV2-eGFP virus. All experiments were performed on cultures at the passages 3–5.

2.6 | RNA extraction and real-time PCR

RNA was extracted from cells by Tripure RNA isolation Reagent (Roche, Germany). Extracted total RNA was reverse-transcribed using Quanti-script reverse transcriptase (Qiagen, Munich, Germany) following the manufacturer's instruction. Corbet Real-Time machine (Applied Biosystems, Munich, Germany) was used for performing quantitative real-time PCR. Experiments were performed using 2× quanti fast SYBER Green (Qiagen) to quantify the mRNA level of SOX2, PAX6, and CHX10, Nestin, rhodopsin, and Thy's-1. Specific primers were purchased from QuantiTect primer assay (Qiagen) (Table 2). In all real-time PCR reactions, β-actin was used as internal control. PCR program included the following three main steps: an initial denaturation step at 95°C for 10 min; 40 cycles of amplification as follows; denaturation (10 s at 95°C), annealing (30 s at 60°C) and finally, extension (15 s at 72°C). To confirm the precision of the reactions, melting curve analysis was performed upon the following steps: step 1, 95.0°C for 0 s; step 2, 65.0°C for 15 s; step 3, 95.0°C for 0 s; step 4, 40.0°C for 30 s. Bio-Rad software (RelQuant UpDate for relative quantification) was used for the calculation of relative gene expression by using $2^{-\Delta\Delta Ct}$ method based on the threshold cycle (Ct) values (Schmittgen & Livak, 2008).

2.7 | Immunocytochemistry (ICC)

Seven days post-infection, SOX2 and eGFP-infected RPE cells were seeded on FBS precoated glass coverslips in 24-well microplates at a density of 1×10^4 cells per well . After 48-hr incubation, standard ICC was performed based on Santa Cruz protocol. Cells were fixed with methanol (−10°C) (Merck) for 5 min and after air-drying, blocking with 1% (w/v) bovine serum albumin (BSA: Sigma, Munich, Germany) in 1% (v/v) PBST (Triton X-100 in PBS) was done for 20 min at room temperature. After the removal of blocking solution, cells were washed with PBS for three times and then overnight incubation in primary antibodies was done at 4°C. All primary antibodies had been diluted 1/200 in BSA 1.5% (w/v)/PBST 1% (v/v). Primary antibodies which were used in this study included: rabbit anti-human polyclonal RPE65 antibody as a specific RPE cell marker, mouse anti-human monoclonal Cytokeratin 8/18 antibody as an epithelial cell marker, rabbit polyclonal anti-human Nestin antibody as neural progenitor cell marker, goat polyclonal anti-human PAX6 and goat polyclonal anti-human CHX10 antibodies as RPC markers, rabbit polyclonal anti-human rhodopsin antibody as photoreceptor cell marker, rabbit polyclonal anti-human THY1 antibody as ganglion cell marker. To avoid non-specific staining, cells were rinsed with PBS for three times, and then incubation in FITC-conjugated antibodies was performed for 45 min at RT in the dark place. Donkey anti-goat for PAX6, SOX2, and CHX10; goat anti-rabbit for Nestin, rhodopsin, and RPE65; goat anti-mouse for Cytokeratin8/18 had been diluted 1/100 in BSA 1.5% (w/v)/PBST 1% (v/v). All antibodies were purchased from (Santa Cruz Company, Brussels, Belgium) (Table 3). For assessing total number of cells in each microscopic field, cell nuclei were counter-stained with DAPI (1 mg/ml, Santa Cruz) for 2 min and then by using mounting

TABLE 2 Primers list which have been used for real-time PCR (Qiagen)

	Catalog number	Primer	Amplicon length (bp)
1	QT00035700	Rho	77
2	QT00023569	Thy1	126
3	QT00071169	PAX	113
4	QT01015301	Nestin	65
5	QT00237601	SOX2	64
6	QT01680476	ACTB	104

TABLE 3 Antibodies list which has been used in this study

Antibody type/ Protein name	Primary antibody	Secondary antibody
Nestin	Rabbit anti human nestin polyclonal antibody Santa Cruz, Sc-20978	Goat anti-rabbit IgG-FITC Santa Cruz, Sc-2012
Pax6	Goat anti human Pax6 polyclonal antibody Santa Cruz, Sc-7750	Donkey anti-goat IgG-FITC Santa Cruz, Sc-2024
Sox2	Goat anti human Sox2 polyclonal antibody Santa Cruz, Sc-17319	Donkey anti-goat IgG-FITC Santa Cruz, Sc-2024
CHX10	Goat anti human Chx10 polyclonal antibody Santa Cruz, Sc-21690	Donkey anti-goat IgG-FITC Santa Cruz, Sc-2024
Thy1	Rabbit anti human Thy1 polyclonal antibody Santa Cruz, Sc-9163	Goat anti-rabbit IgG-FITC Santa Cruz, Sc-2012
Rho	Rabbit anti human Rho polyclonal antibody Santa Cruz, Sc-20193	Goat anti-rabbit IgG-FITC Santa Cruz, Sc-2012
Cytokeratin 8/18	Mouse anti human cytokeratin8/18 monoclonal antibody Santa Cruz, Sc-52325	Goat anti-mouse IgG-FITC Santa Cruz, Sc-2010
RPE65	Rabbit anti human RPE65 polyclonal antibody Santa Cruz, Sc-32893	Goat anti-rabbit IgG-FITC Santa Cruz, Sc-2012

media (glycerol 90%, PBS 10%, phenyl diamin 10% [w/v]), coverslips were mounted on slides. Axiophot Zeiss fluorescence microscope (Germany) equipped with a 520 nm filter for FITC and a 460 nm filter for DAPI was used to observe slides. Controls applied in this test included a background control with no antibody (neither primary nor secondary) and a secondary antibody-only control for assessing specification of primary antibody.

2.8 | Statistical analysis

Experiments were performed in at least three independent repeats and the number of repetitions for each sample was at least two times in each experiment. Student's *t*-test was used to evaluate the statistical significance of the data; *p*-value of <0.05 was considered as being statistically significant.

3 | RESULTS

3.1 | Production of recombinant AAV2 particles

Microscopic examination of transfected HEK293T cells after 48 hr verified GFP expression. Seventy-two hours post-transfection, hallmarks of virus production were monitored. As viral production proceeded, some of the cells rounded up and detached from the culture surface and floated in the medium (data not shown).

Flow cytometry data confirmed titer of 1.8×10^8 particles/ml for purified and concentrated AAV2-eGFP virus and 0.5×10^8 particles/ml for rAAV2-SOX2-GFP virus (Figure 1).

In comparison to flow cytometry, quantitative PCR data for virus tittering showed 3.3×10^{12} g DNA/ml for AAV2-eGFP and 2.5×10^{12} g particles/ml for rAAV2-SOX2-GFP.

3.2 | RPE cell culture establishment and characterization

Human neonatal RPE cells attached to the culture surface 24 hr after the beginning of primary culture. Neonatal RPE cells underwent different morphological changes. As shown in Figure 2. In the first days of culture, cells were small and revealed fusiform shapes (Figure 2a). Cells increased in size and acquired fibroblast-like morphology through repeated passages, also pigmentation decreased gradually (Figure 2b). Cobblestone structures were observed when the cultures formed monolayer and became full confluent (Figure 2c). RPE cells usually after the 10th passage flattened and lost their proliferative ability (Figure 2d).

Twenty-four hours after the beginning of the culture, isolated human adult RPE cells presented small, spherical dark morphology (Figure 2e) but 3 days later, although the cells were still pigmented, they took fusiforms shapes in culture (Figure 2f). By passing the time, large colonies were found in some culture vessels (Figure 2g). Adult human RPE cells in the second passage (Figure 2h) showed the birth of giant colonies (Figure 2i). RPE spheroids were, then, detached and suspended in the supernatant (Figure 2j). Fully pigmented colonies, partially pigmented colonies, or non-pigmented colonies were detected in adult hRPE cultures.

ICC test was performed in newly isolated RPE cells for RPE65, RPE specific marker, cytokeratin8/18 as epithelial cell marker and ZO-1, tight junction protein. Nearly all of the isolated cells represented the aforesaid markers and the identity and purity of cultures, as RPE, were confirmed (Figure 3).

3.3 | Neural/RPC marker expression in infected RPE cells

Based on time study results, human neonatal/adult RPE cells were infected with rAAV2-SOX2-GFP and control virus (MOI = 10). Then SOX2 and

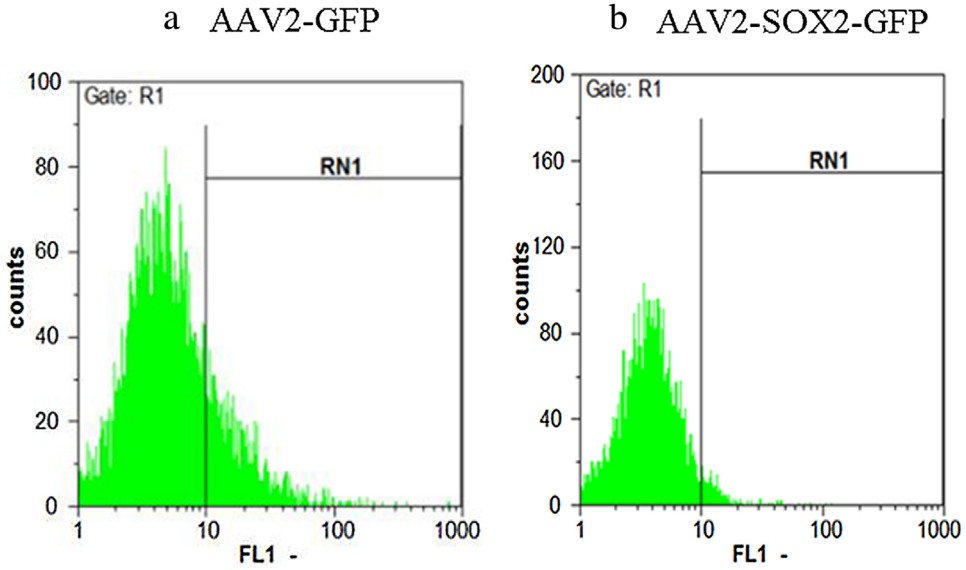

FIGURE 1 Flow cytometry of HEK293T cells, which had been infected by AAV2-GFP and AAV2-SOX2-GFP; Functional titration of viral preparations. Flow cytometry histogram of (a) AAV2-GFP and (b) AAV2-SOX2-GFP stocks that determines infectious particles titer. The histograms show expression of GFP and the number of functional AAV2-SOX2-GFP particles which infected HEK293T cells. Data were analyzed 48 hr post-infection

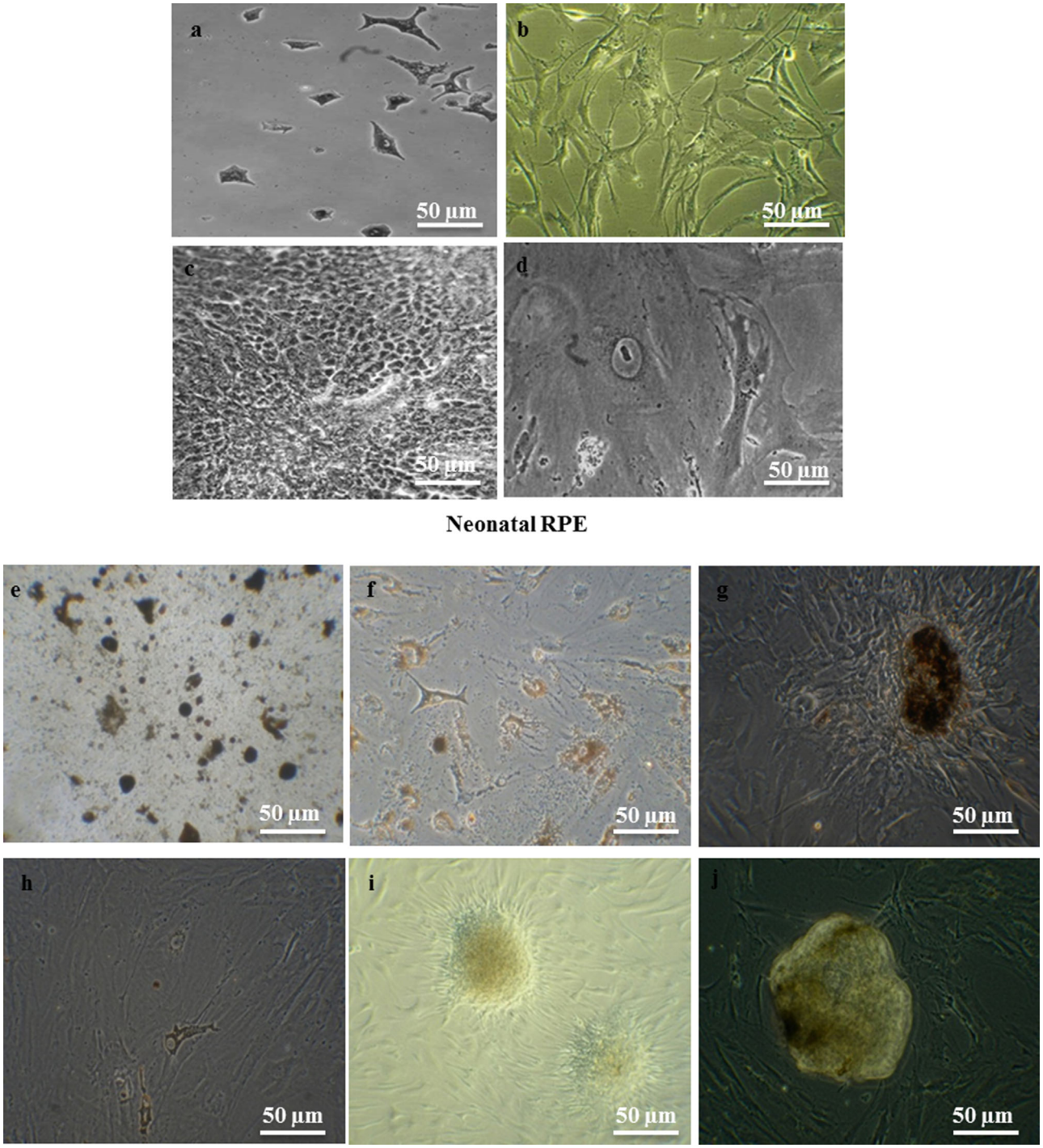

FIGURE 2 Retinal pigment epithelium (RPE) cells in primary culture. (a) Freshly isolated RPE cells from human new born eye. (b) RPE cells acquired their typical fibroblast-like morphology in in vitro cultures. (c) Formation of cobblestone structures in a monolayer of confluent RPE cells. (d) Flattened RPE cells in an aged culture. 200×. (e) Human adult RPE cells twenty-four hours after the beginning of the culture, isolated cells presented small, spherical dark morphology. (f) Three days later, the cells were still pigmented and took fusiforms shapes. (g) The appearance of colony in culture. (h) RPE cells in the second passage. (i) The birth of giant colonies in culture. (j) RPE spheroids were detached and suspended in the supernatant; in a giant colony several cells lost their pigments while the others maintained the brown pigmentation. 200×

neural/RPCs' marker expression was analyzed in infected and control cultures of neonatal/adult hRPE (Figure 4).

Time study experiment showed that 24 hr post-infection was the optimum time for the detection of SOX2 over-expression in infected neonatal hRPE cells (data not shown). Relative gene expression analysis showed up to 80-fold over-expression for SOX2 gene and 3.8- and 3-fold increase in the expression of Nestin and PAX6 markers in treated neonatal hRPE cells in

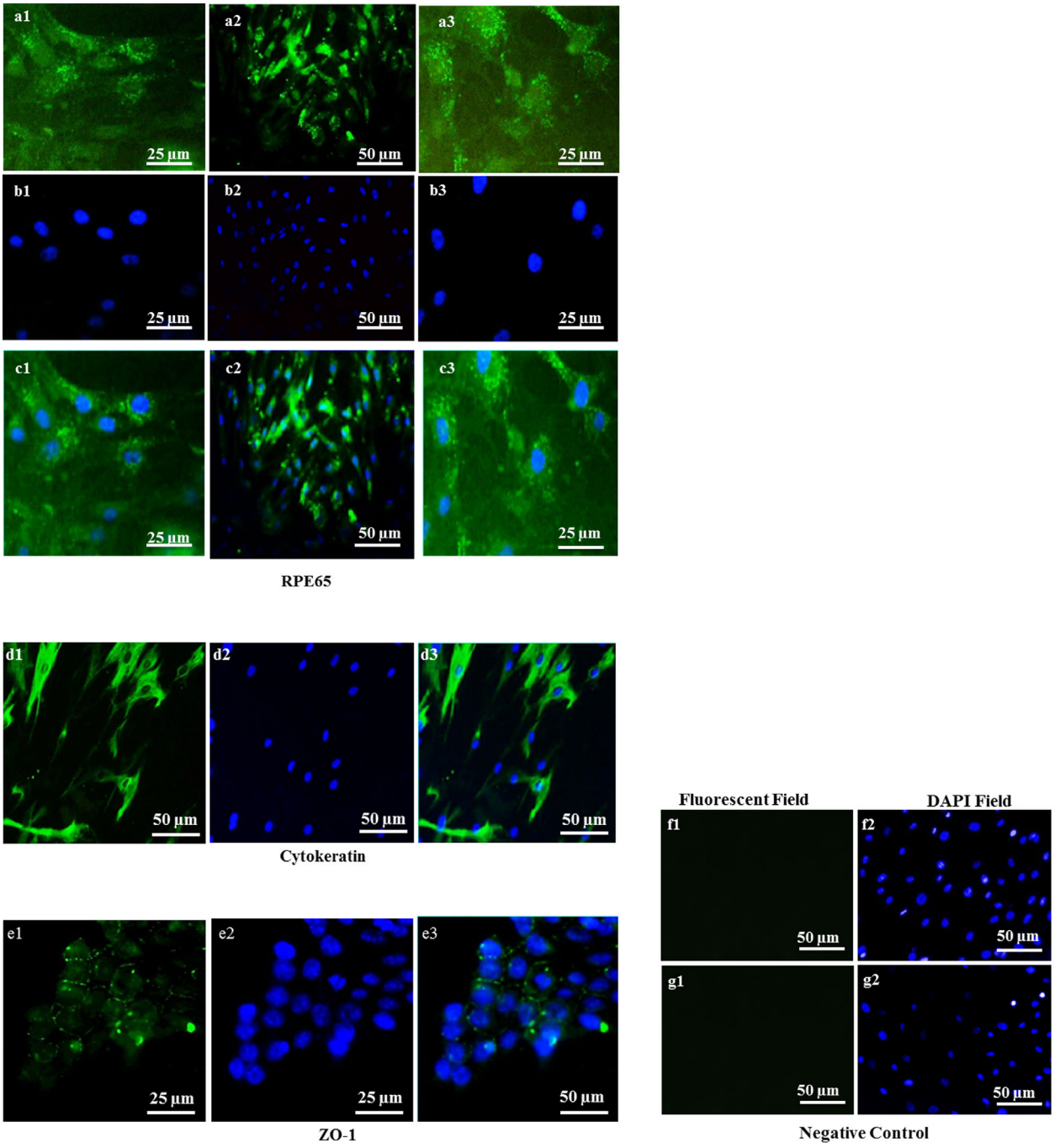

FIGURE 3 Characterization of isolated cells by RPE specific markers (a1) Microsomal and cytoplasmic expression of RPE65. Three different microscopic fields in different magnifications have been shown (a1 and a3: 400×, a2: 200×). (b1-3) Staining of the cells' nuclei in (a) with 4′, 6-diamidino-2-phenylindole dihydrochloride (DAPI). (c) Merg of (a) and its related (b) image. (d1) Cytoplasmic expression of cytokeratin 8/18 confirmed the epithelial identity of the cells. (d2) Staining of the cells' nuclei in (d1) with DAPI. (d3) Merg of (d1) and (d2). (e1) Immunofluoresence image of ZO-1 in cultured cells. (e2) Staining of the cells' nuclei in (e1) with (DAPI). (e3) Merg of (e1) and (e2). 400×. (f1 and g1) ICC for cell cultures without using primary antibodies, as negative controls. (f2 and g2) Dapi staining of cells' nuclei in control cultures. 200×

comparison to control cells which were infected by AAV2-GFP virus (Figure 4a).

Adult hRPE cells' culture was also infected by AAV2 harboring SOX2. Although 24 hr post infection was the optimum time for chasing SOX2 overexpression in neonatal hRPE cells and SOX2 expression was increased 80-fold, we detected 3.5–12-fold increase in SOX2 expression in adult hRPE cells after 48 hr (Figure 4b).

Nestin and PAX6 expression was increased 3.5- and 2.5-fold, respectively, in treated adult hRPE cells. Howbeit, we could not detect

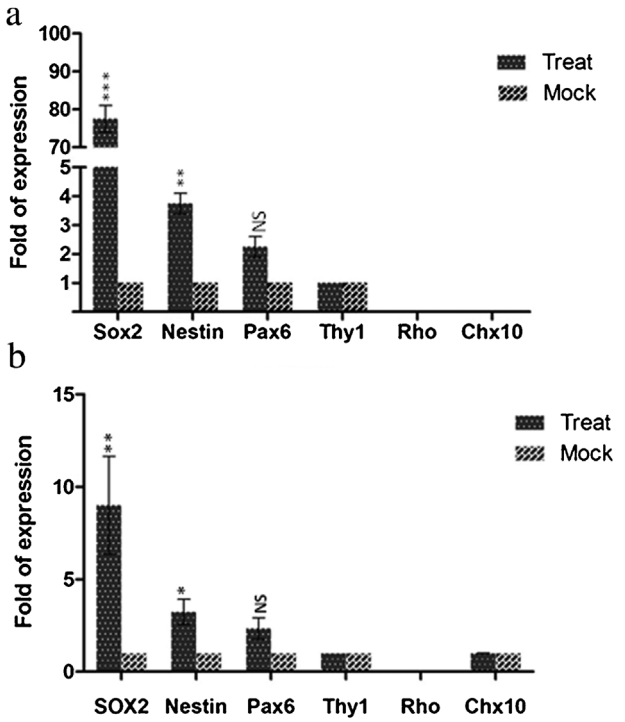

FIGURE 4 (a) Bar graphs are showing expression of SOX2, Nestin, PAX6, Thy1, rhodopsin, and CHX10 in infected neonatal hRPE cells. 24 hr/48 hr post-infections, total RNAs were extracted from neonatal hRPE cells and real-time PCR performed using specific primers. The expression levels were normalized with cultures that had been infected by AAV2-GFP virus. Data showed alongside SOX2 overexpression (80-fold), Nestin and PAX6 expression was increased 3.8- and 3-fold, respectively. However, Thy1 expression remained relatively unchanged and rhodopsin (Rho) and CHX10 were not detected in mRNA transcript level. Significance was determined with unpaired Student's *t*-test by comparing each time point with cultures that had been infected by AAV2-GFP. Error bars represent standard error of the mean. ***$p < 0.0005$, **$p < 0.0005$ NS: non-significant, RPE: retinal pigmented epithelium. (b) Bar graphs are showing expression of SOX2, Nestin, PAX6, Thy1, rhodopsin, and CHX10 in infected adult hRPE cells. Data showed 3.5–12-fold increase in SOX2 expression in adult derived cells 48 hr post-infections. Assessment of gene expressions for Nestin, PAX6, Thy1, rhodopsin, CHX10 revealed that solely Nestin and PAX6 expression was increased 3.5- and 2.5-fold, respectively (Figure 4b) rhodopsin expression was not detected in adult hRPE cultures, Thy1 and CHX10 steady expression were confirmed in both AAV2-SOX2-GFP treated and control adult hRPE cells. Significance was determined with unpaired Student's *t*-test by comparing each time point with RPECs that had been infected by AAV2-GFP. Error bars represent standard error of the mean. **$p < 0.005$, *$p < 0.05$, NS: non-significant, RPE: retinal pigmented epithelium. The analysis was performed using three independent biological samples ($n = 3$) in duplicate and the comparative cycle threshold ($2^{-\Delta\Delta Ct}$) method was used to determine relative changes in transcripts compared with ACTB mRNA levels

rhodopsin and CHX10 expression in neonatal hRPE cultures and rhodopsin expression in adult hRPE cells.

Thy1 steady expression was confirmed in both treated and control hRPE cells which had been derived from both neonatal and adult globes (Figure 4a,b).

3.4 | Immunocytochemistry assessment of retinal cells' markers

Pursuing aforesaid markers' proteins' expression by ICC showed that almost 25% and 30% of the neonatal and adult hRPE cells were positive for SOX2 nuclear expression after transduction by AAV2-SOX2-GFP viral particles, while this value was only 5% in controls (Figure 5a–c).

Nuclear expression of retinal stem/progenitor cells' markers, PAX6 and CHX10, was observed in 10% and 5% of treated neonatal cells, respectively (Figure 5d–i). While just 2% of control cells detected with nuclear localization of positive signals. Nevertheless, we detected PAX6 diffused cytoplasmic expression in treated neonatal human RPE cells, something that we had not find before (Figure 5g4).

Adult hRPE cells were 35% and 12% positive for PAX6 and CHX10 after SOX2 overexpression (Figure 5d–i). Corresponding controls, which had been infected with AAV2-GFP, showed only 2% and 5% positive cells for PAX6 and CHX10, respectively.

Approximately 40% and 50% of cells in neonatal and adult hRPE infected cultures expressed Nestin, respectively, while only 1–5% of control cells expressed this neurofilament protein (Figure 5j–l).

Neonatal-derived hRPE cell cultures revealed 2% Thy1 and 2% rhodopsin positive cells. These values were 45% and 30% for the adult hRPE-treated cultures (Figure 5m–r). In control cultures (treated by AAV2-GFP), an ignorable number of cells were positive for Thy1 and rhodopsin (about 5%).

3.5 | DISCUSSION

Retina is subjected to various degenerative diseases like AMD which results from photoreceptors destruction and glaucoma that affect retinal ganglion cells (Lamba et al., 2008). Because of degeneration and death of RPE cells, photoreceptors and other retinal neurons are the most important reasons of retinal diseases. Substituting degenerated cells by cell therapy is a promising treatment that currently is in hand. The choice of an appropriate cell source is a critical point in cell therapy. RPE cells, regarding the anatomical proximity to the photoreceptors and common developmental origin with neural retina, draw many researcher's attention for cell therapy. Many studies have shown trans-differentiation of RPE to neural/RPCs by transcription factors and small molecules augment (Davari et al., 2013; Lamba et al., 2008). Very recently Saini, Temple, and Stern (2016) reported hRPE as a promising source for retinal stem cells (RPESC).

Since gene expression may prevent irreversible pathological events, many reports suggest that there are numerous advantages for initiating gene therapy in the neonates rather than adults. In the neonates life, the earlier vector administration; then the greater vector to cell ratio and therefore the less vector administration. Moreover stem and progenitor cells that are likely less accessible later in life are more easily transduced and finally the immune responses may be reduced or absent in neonates (Hu, Busuttil, & Lipshutz, 2010).

In the study ahead, we investigated the impact of rAAV2-mediated SOX2 delivery into neonatal human RPE cells in comparison with human adult RPE cells.

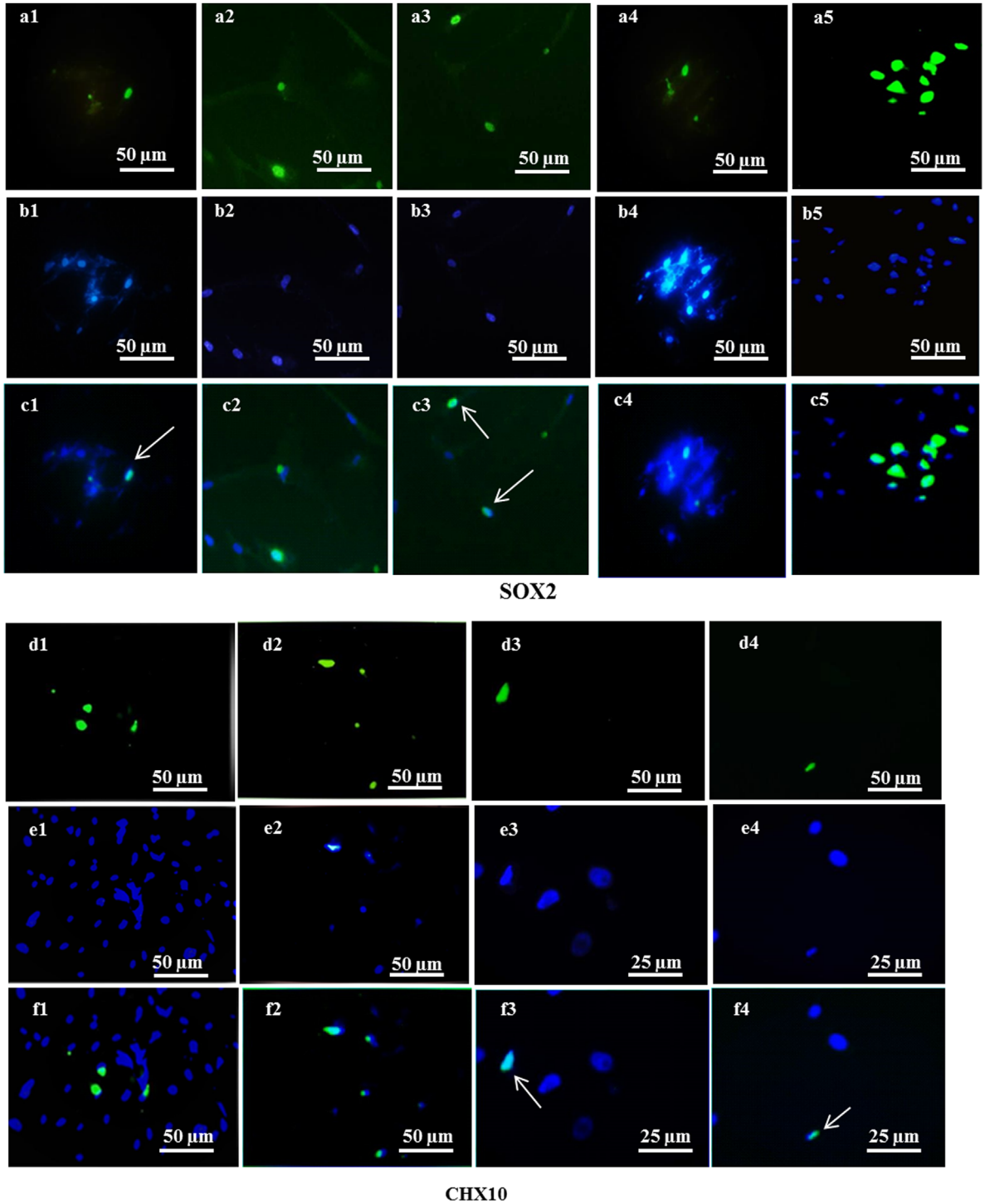

FIGURE 5 Protein expression of SOX2, Nestin, PAX6, Thy1, rhodopsin, and CHX10 in SOX2-treated human RPE cells. Neonatal/adult hRPE cells were infected with AAV2-SOX2-GFP or AAV2-GFP virus (as control) and 7 days post-infection were seeded on FBS pre-coated glass coverslips in 24-well microplates. After 48 hr, ICC was performed. a1-5) ICC for SOX2. b1-5) Corresponding DAPI of (a) images. c1-5) Merge of (a) and its related (b) image. d1-4) ICC with antibody against CHX10 and e1-4) its corresponding DAPI. f1-4) Merge of (d) and its related (e) image. g1-4) Nuclear and perinuclear cytoplasmic localization of PAX6 and h1-4) its corresponding DAPI. (g4) Cytoplasmic expression of PAX6 in neonatal hRPE cells which had been treated with AAV2-SOX2-GFP. Note to that neurite projections which was detected by arrow and compare it with G3 that represents cytoplasmic expression of Pax6 which has been found only in SOX2-treated, adult RPECs cultures. i1-4) Merge of (g) and its related (h) image. j1-3) Expression of Nestin in SOX2-treated RPE cells and k1-3) its corresponding DAPI. (j3 and k3 400X). l1-3) Merge of (j) and its related (k) image. m1-2) ICC for rhodopsin and n1-2) its corresponding DAPI. o1-2) Merge of (m) and its related (n) image. p1-2) Thy1 (retinal ganglion cell marker) expression in SOX2-treated cells and q1-2) its corresponding DAPI. r1-2) Merge of (p) and its related (q) image. Photographs are representative pictures that have been taken from at least three independent experiments, 200×

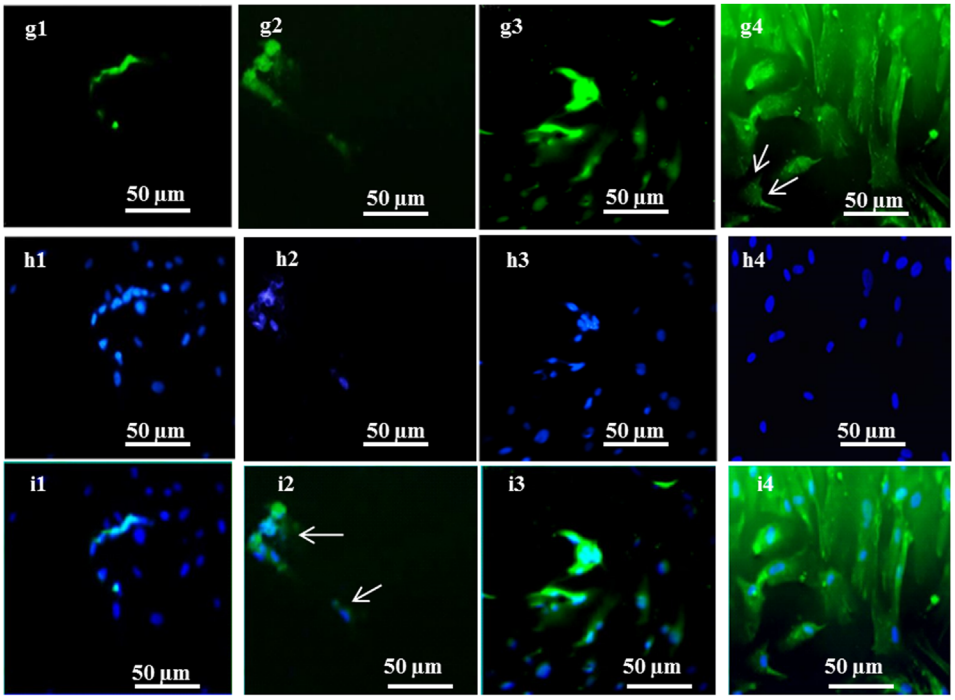

Pax6

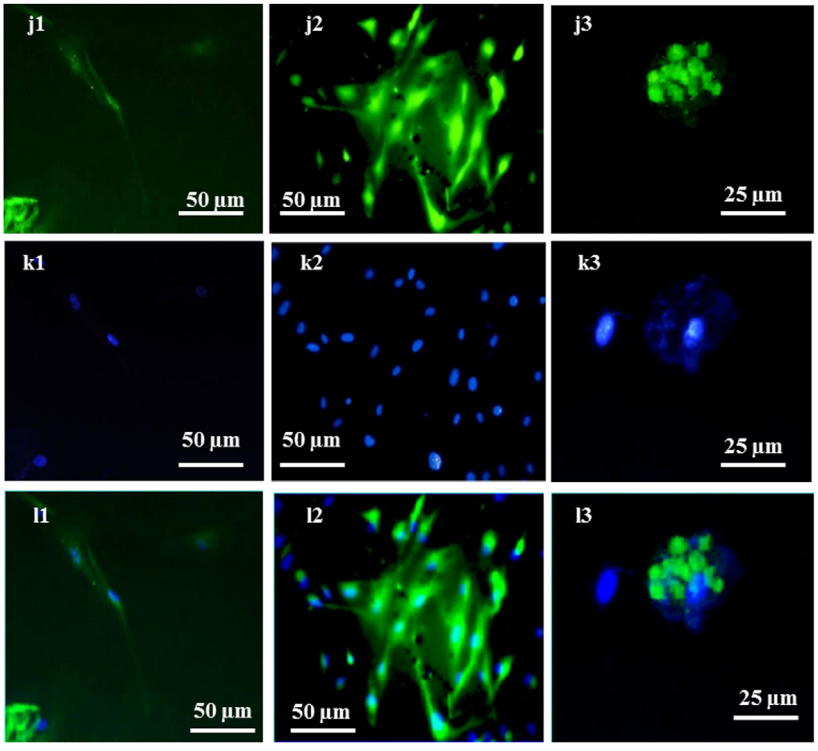

Nestin

FIGURE 5 Continued.

Although the rate of successful cultures was nearly 100% for neonatal-derived RPE, there was a reverse relationship between the donor's age and the viability of the culture for adult-derived RPE cultures, so that solely 50–70% of the trials ended with a successful culture.

Neonatal and adult hRPE cells showed, nearly, the similar morphological changes in their in vitro establishing processes. However, adult cells looked more pigmented and represented a clear brownish color even with unaided visualizations of the cultures. They also much earlier reached to the senescence phase when compared with neonatal RPE-derived cells.

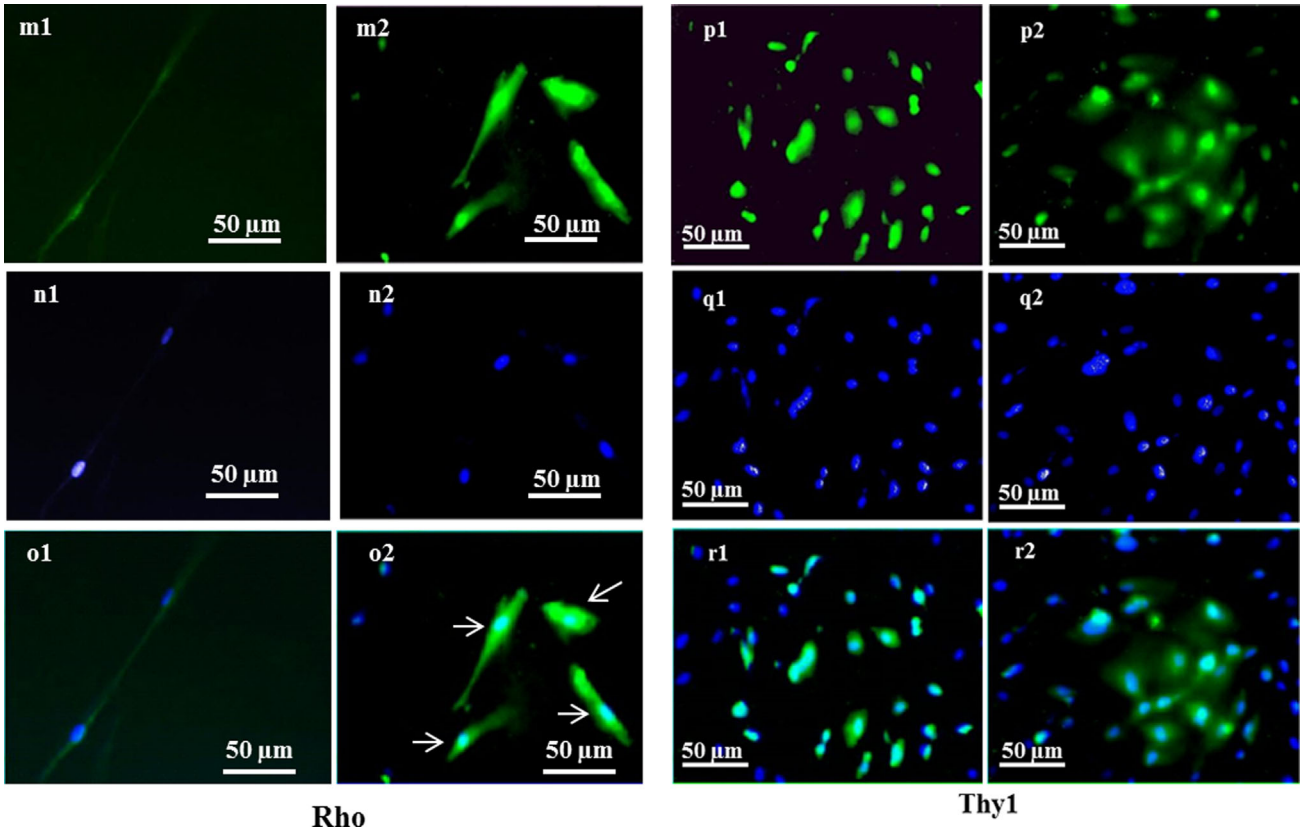

FIGURE 5 Continued.

The appearance of differently pigmented spheroid colonies that gradually detached from the substrate and floated in supernatant indicated the presence of sub-populations of hRPE cells that had been dedifferentiated and turned into stem cells.

Time study results showed that 24 hr post-infection transgene over-expression was significant in neonatal hRPE cells. Since human neonatal RPE cells exhibited high proliferative ability in culture (doubling time around 25 hr), loss of episomal genome occurred with rapid cell division and concomitantly increased gene expression declined rapidly. However, unlike neonatal hRPE cells, the optimum time for transgene expression was around 48 hr post-infection in adult hRPE-derived cultures and remained substantially constant up to 65 hr post-infection (data not shown). These disparities may be imputed to slower cell kinetic in adult-derived cells (doubling time about 50 hr). Again studies have demonstrated that in adult animals, AAV2 transgene expression is characterized by a lag phase presumably due to a postponement in un-coating and transformation of single-stranded vector genomes by second strand synthesis; this can be up to 5 weeks with AAV2 (Miao et al., 1998; Thomas, Storm, Huang, & Kay, 2004).

Furthermore, the highest fold of increase in transgene expression was detected for neonatal cells (80-fold with respect to 12-fold for adult cells). One explanation for the distinct differences in transgene fold of increase may be due to existing differences in initial transduction and variation in kinetics of viral uncoating and indicated that high-levels of transduction are possible with AAV2 for neonatal hRPE gene transfer.

According to time study result, gene over-expression was analyzed 24 hr/48 hr post-infection in neonatal/adult hRPE cells, respectively, and significant expression of SOX2 and Nestin was observed by real-time PCR and ICC. According to the previous studies, SOX2 binds to an enhancer region of Nestin gene and increases its expression, so it seems that our result was consistent with the previous studies (Tanaka et al., 2004). Since Nestin is a neural progenitor cell marker (Lee, Park, Shin, Chun, & Oh, 2012; Wiese et al., 2004), its expression in SOX2-transduced cells suggests that SOX2 over-expression could drive RPE cells toward neural progenitor cells. Based on the study by Taranova et al. (2006), SOX2 is critical for the maintenance of neural progenitor cells' identity in retina, so that decline in SOX2 expression in developing retina culminates in decreased proliferative ability of the cells. In addition, a direct relationship between SOX2 and Notch1 gene was found in Taranova study, Notch signaling maintains undifferentiated state of stem cells by inhibiting neurogenesis. According to Shih and Holland (2006), Notch signaling activates Nestin promoter and Nestin expression and therefore may result in the maintenance of stemness properties. Thus, according to the previous studies, and our study, it can be concluded that SOX2 over-expression in neonatal/adult hRPE cells triggers Notch1 signaling and subsequently Notch1 activates Nestin as neural progenitor marker.

Previous studies showed that the balance in the levels of SOX2 regulates the choice between maintenance of RPC identity and/or differentiation routs (Taranova et al., 2006).

In our study, a low rise in the expression of PAX6 RPC marker was observed in SOX2-transduced neonatal/adult hRPE cells. On the basis of the study by Hsieh and Yang (2009), PAX6 shows dynamic expression during the retinal progenitors' cell cycle such that a significant downregulation in PAX6 protein observed as progenitors undergo the preneurogenic to neurogenic transition (Hsieh & Yang, 2009). Low rise in PAX6 expression in neurogenic period, which is associated with high level of SOX2 expression, is critical for proliferation, survival, and specification of progenitor cells. So neurogenic progenitors maintain low PAX6 level during the S phase and proliferate. Then, in a subset of retinal progenitors, PAX6 level rapidly increases or decreases as the cells enter G2/M phase of the cell cycle. According to the study by Matsushima, Heavner, and Pevny (2011), the functional contradiction between SOX2 and PAX6 is indispensable for reasonable patterning of the eyecup, and SOX2 and PAX6 are expressed in a vice versa fashion. In accordance with the previous reports, our results showed 24 hr/48 hr post-infection (in neonatal/adult hRPE cells respectively) was associated with high levels of SOX2 expression, while PAX6 expression level, which is crucial for progenitor cell proliferation, was slightly increased. Hsieh and Yang (2009) showed that the expression of PAX6 increases in a subset of progenitor cells at the end of S phase of cell cycle.

Moreover, treated neonatal hRPE cultures revealed a plenty of cytoplasmic PAX6+ cells, something that we did not observe previously. Cytoplasmic PAX6 usually is expressed in outer nuclear cell layer (Shin et al., 2003). It has an early role in morphogenesis and cell migration, and a distinct later function in retinal neurogenesis. It is a pan amacrine cell marker and induces formation of neurite projections (Philips et al., 2005).

Cytoplasmic PAX6+ cells presumably represent amacrine/RGC cells with neurite projections and distinct morphology in treated neonatal hRPE cultures.

We could not detect the expression of CHX10 in infected neonatal hRPE cells 24 hr post-infection, while ICC data confirmed its protein expression 7 days post-infection (although there were no significant changes in the number of positive cells between treated and controls). Based on the study by Dhomen et al. (2006), lack of CHX10 expression during the progenitor cell cycle leads to the propagation of progenitor cells. Furthermore, CHX10 is a marker of bipolar cells and its expression in ICC suggests a newly occurred trans-differentiation toward bipolar cells. Additional analysis of bipolar markers should be carried out to confirm this.

Although CHX10 transcripts were detected in adult hRPE-derived cells, it remained unchanged in AAV2-SOX2-GFP-infected cells when compared to control. ICC revealed a sizeable number of CHX10+ cells in treated adult hRPE cells.

Taken together, the above results showed that both the PAX6 and CHX10 proteins were significantly increased in adult hRPE-derived cells with respect to its neonatal counterpart. The coincidental increase of PAX6 and CHX10 with Nestin in the aforesaid cells may point to the existence of a more primitive stem cells/progenitor cells in SOX2-treated adult hRPE cultures.

Expression of rhodopsin was not detected in mRNA transcript level, in all performed experiments, while 2% and 30% of SOX2-infected neonatal/adult hRPE cells expressed rhodopsin in ICC. Just like our study, expression of rhodopsin has been previously shown at protein level but not at mRNA transcript level in RPE cell cultures (Bibb et al., 2001).

We also assayed SOX2-transduced cells for expression of Thy1 as retinal ganglion cell marker and confirmed that 2% and 45% of SOX2-infected neonatal/adult hRPE cells expressed Thy1 in ICC. It revealed that adult hRPE-derived cells generated fully differentiated retinal cells when they were transduced with AAV2-SOX2-GFP viruses. This occurred while the level of Thy1 transcripts remained unchanged. This indicates that Thy1 protein expression was regulated post-transcriptionally in the aforesaid cells.

Prominent presence of rhodopsin+ cells and Thy1+ cells, in treated adult human RPE cultures, determined considerable progress of reprogramed adult hRPE cells toward neuro-retinal terminally differentiated cells.

The sum of percentages of Nestin-positive cells (neural progenitors, 50%), Thy1-positive cells (ganglion cells, 45%), rhodopsin-positive cells (photoreceptor cells, 30%) in virus-infected adult RPE cells is over 100%. Since many mature retinal cell types, including RGCs, are derived from multipotent RPCs (Gill, Hewitt, Davidson, Pébay, & Wong, 2014), it seems that some of the cells expressed both Nestin and Thy1 and therefore were counted twice in quantification of ICC results.

Moreover when cultured RPCs are treated with RA, RPC cells exhibit Nestin co-expression with various retinal specific markers, including protein kinase C α (PKC), neurofilament 200 (NF200), cellular retinaldehyde binding protein (CRALBP), and rhodopsin (Qiu et al., 2007). So again, in our results, a subpopulation of RPCs probably expressed both Nestin and rhodopsin. These cells have also been counted twice. It has also been shown that the primitive RPCs will culminate in terminally differentiated functionally active retinal cells through an allied process in which a differentiating cell transiently express both pluripotency markers and differentiation markers simultaneously (Kallas, Pook, Trei, & Maimets, 2014). This would be another explanation for over 100% counts in aforesaid ICC experiments.

It has been previously demonstrated that cellular senescence affects the reprogramming efficiency of induced pluripotent stem cells (Banito et al., 2009; Kawamura et al., 2009; Li et al., 2009), and age, through the activation of the p21 and p16 pathways, induces cell cycle arrest (Campisi & Di Fagagna, 2007; Narita et al., 2003). Accordingly, the inherent properties of somatic cells designate the reprogramming efficiency and cellular fate.

In murine cells, donor age has an obvious effect on reprogramming efficiency (Wang et al., 2011). Unlike what has been reported in mice, donor age does not seem to impair the reprogramming efficiency of human cells (Somers et al., 2010).

In accordance with Somers et al. (2010), the data presented here revealed that the age would presumably not be the determinative factor in the cellular fate of reprogramed hRPE cells. Adult/neonatal hRPE cells, reprogramed by AAV2-SOX2, culminated in cultures that were boosted by retinal stem cells/progenitor cells. The only important difference was that neuroretinal terminally differentiated cells were mostly detected when the origin of utilized hRPE cells was the adults' globes. It remains to be answered whether there is a type of crosstalk between the population of original hRPE cells and the reprogramed hRPE cells that determine the final cellular fate.

The exploitation of stem cells in regenerative medicine requires a deep understanding of developmental biology and key regulators in the retinal cell differentiation pathways. Somatic cells can also be reprogramed to related lineages by overexpression of well-known transcription factors.

Identification of the prospects that each type of cells might offer is a critical concern. Specifically, assessment of the outcomes of transplantation experiments, including identification of the cell types generated and their impact on visual function, is too important (MacLaren & Pearson, 2007).

Although most reprogramming has been performed by using fibroblast cells, they are not easily reprogramable. Additionally, the biopsy procedure is invasive. So another cell types have also been used for reprogramming (Aasen et al., 2008; Giorgetti et al., 2009).

Efficiency and easiness of reprogramming depend on donor cell types. This is due to endogenous expression of specific transcription factors (Kim et al., 2010) in recruited cells.

This would be worthwhile to use the cell types which share the same origin of the interested tissue (Hu et al., 2014).

Normal RPE cells in newts can transform into retinal neurons and ganglion cells. Therefore, they can serve as a model to identify factors of the competence of vertebrate cells for reprogramming in vivo (Grigoryan & Markitantova, 2016).

Guiding non-neural RPE to produce retinal neurons offers a source for cell-replacement of developing neurons. Sox2 plays important roles in maintaining neural progenitor/stem cell properties and in converting fibroblasts into pluripotent stem cells (Ma et al., 2009).

In this study, we used AAV2 to deliver SOX2 gene to human retinal pigmented epithelial, hRPE, cells. We demonstrated that hRPE cells can be directly reprogramed to retinal stem/progenitor cells and concomitantly neuroretinal terminally differentiated cells depending on the neonatal or adult origin of utilized RPE cells by introduction of SOX2.

Many degenerative diseases of the retina are associated with age. Moreover recruitment into the clinical phase of gene therapy requires many considerations. The patient's age is one of the most important factors that influence the outcome of gene therapy which should be considered. So the in vitro and pre-clinical study which considers the age of volunteers is essential (Herzog, Cao, & Srivastava, 2010). A trial in children showed that the extent of visual improvement achieved by the gene therapy is age-dependent (Maguire et al., 2009).

Tissue engineering and cell replacement therapy are becoming more established therapeutic interventions for retinal degenerative diseases. Stem cells in the treatment of retinal disorders represented an encouraging source for transplantation but the loss of reasonable quantity of relevant RPE cells and the current disputes on the issue of stem cell applications have created obstacles with regard to achieving qualified sources of cells for transplantation. RPCs, if available, can offer the most impressive setting for transplantation.

The current study showed that hRPE cells, reprogramed by AAV2-SOX2-GFP, have the potential to generate retinal stem cells/progenitor cells and concomitantly neuroretinal terminally differentiated cells depending on the neonatal or adult origin of utilized RPE cells.

REFERENCES

Aasen, T., Raya, A., Barrero, M. J., Garreta, E., Consiglio, A., Gonzalez, F., . . . Tiscornia, G. (2008). Efficient and rapid generation of induced pluripotent stem cells from human keratinocytes. *Nature Biotechnology*, *26*, 1276–1284.

Banito, A., Rashid, S. T., Acosta, J. C., Li, S., Pereira, C. F., Geti, I., . . . Walsh, M. (2009). Senescence impairs successful reprogramming to pluripotent stem cells. *Genes & Development*, *23*, 2134–2139.

Bibb, L. C., Holt, J. K., Tarttelin, E. E., Hodges, M. D., Gregory-Evans, K., Rutherford, A., . . . Gregory-Evans, C. Y. (2001). Temporal and spatial expression patterns of the CRX transcription factor and its downstream targets. Critical differences during human and mouse eye development. *Human Molecular Genetics*, *10*, 1571–1579.

Blenkinsop, T. A., Salero, E., Stern, J. H., & Temple, S. (2013). The culture and maintenance of functional retinal pigment epithelial monolayers from adult human eye. *Epithelial Cell Culture Protocols: Second Edition*, *945*, 45–65.

Campisi, J., & Di Fagagna, F. D. A. (2007). Cellular senescence: When bad things happen to good cells. *Nature Reviews Molecular Cell Biology*, *8*, 729–740.

Cepko, C. (2014). Intrinsically different retinal progenitor cells produce specific types of progeny. *Nature Reviews Neuroscience*, *15*(9), 615–627.

Chen, M., Chen, Q., Sun, X., Shen, W., Liu, B., Zhong, X., . . . Chai, F. (2010). Generation of retinal ganglion-like cells from reprogrammed mouse fibroblasts. *Investigative Ophthalmology & Visual Science*, *51*, 5970–5978.

Davari, M., Soheili, Z.-S., Ahmadieh, H., Sanie-Jahromi, F., Ghaderi, S., Kanavl, M. R., . . . Javidi-Azad, F. (2013). Amniotic fluid promotes the appearance of neural retinal progenitors and neurons in human RPE cell cultures. *Molecular Vision*, *19*, 2330.

Dhomen, N. S., Balaggan, K. S., Pearson, R. A., Bainbridge, J. W., Levine, E. M., Ali, R. R., & Sowden, J. C. (2006). Absence of chx10 causes neural progenitors to persist in the adult retina. *Investigative Ophthalmology & Visual Science*, *47*, 386–396.

Ferri, A. L., Cavallaro, M., Braida, D., Di Cristofano, A., Canta, A., Vezzani, A.,. . . Debiasi, S. (2004). Sox2 deficiency causes neurodegeneration and impaired neurogenesis in the adult mouse brain. *Development*, *131*, 3805–3819.

Fuhrmann, S., Zou, C., & Levine, E. M. (2014). Retinal pigment epithelium development, plasticity, and tissue homeostasis. *Experimental Eye Research*, *123*, 141–150.

Gill, K. P., Hewitt, A. W., Davidson, K. C., Pébay, A., & Wong, R. C. (2014). Methods of retinal ganglion cell differentiation from pluripotent stem cells. *Translational Vision Science & Technology*, *3*, 2–2.

Giorgetti, A., Montserrat, N., Aasen, T., Gonzalez, F., Rodríguez-Pizà, I., Vassena, R., . . . Corbella, B. A. (2009). Generation of induced pluripotent stem cells from human cord blood using OCT4 and SOX2. *Cell Stem Cell*, *5*, 353.

Grigoryan, E. N., & Markitantova, Y. V. (2016). Cellular and molecular preconditions for retinal pigment epithelium (RPE) natural reprogramming during retinal regeneration in urodela. *Biomedicines*, *4*, 28.

Herzog, R. W., Cao, O., & Srivastava, A. (2010). Two decades of clinical gene therapy—Success is finally mounting. *Discovery Medicine*, *9*, 105.

Hsieh, Y.-W., & Yang, X.-J. (2009). Dynamic Pax6 expression during the neurogenic cell cycle influences proliferation and cell fate choices of retinal progenitors. *Neural Development*, *4*, 8104–8104.

Hu, C., Busuttil, R. W., & Lipshutz, G. S. (2010). RH10 provides superior transgene expression in mice when compared with natural AAV serotypes for neonatal gene therapy. *The Journal of Gene Medicine*, *12*, 766–778.

Hu, Q., Chen, R., Teesalu, T., Ruoslahti, E., & Clegg, D. O. (2014). Reprogramming human retinal pigmented epithelial cells to neurons using recombinant proteins. *Stem Cells Translational Medicine*, *3*, 1526–1534.

John, S., Natarajan, S., Parikumar, P., Shanmugam, P. M., Senthilkumar, R., Green, D. W., & Abraham, S. J. (2013). Choice of cell source in cell-based therapies for retinal damage due to age-related macular degeneration: A review. *Journal of Ophthalmology*, *2013*, 465169.

Kallas, A., Pook, M., Trei, A., & Maimets, T. (2014). SOX2 is regulated differently from NANOG and OCT4 in human embryonic stem cells during early differentiation initiated with sodium butyrate. *Stem Cells International*, *2014*, 298163.

Kawamura, T., Suzuki, J., Wang, Y. V., Menendez, S., Morera, L. B., Raya, A.,... Belmonte, J. C. I. (2009). Linking the p53 tumour suppressor pathway to somatic cell reprogramming. *Nature*, *460*, 1140–1144.

Kim, K., Doi, A., Wen, B., Ng, K., Zhao, R., Cahan, P., ... Ehrlich, L. (2010). Epigenetic memory in induced pluripotent stem cells. *Nature*, *467*, 285–290.

Lamba, D., Karl, M., & Reh, T. (2008). Neural regeneration and cell replacement: A view from the eye. *Cell Stem Cell*, *2*, 538–549.

Lee, J. H., Park, H. S., Shin, J. M., Chun, M. H., & Oh, S. J. (2012). Nestin expressing progenitor cells during establishment of the neural retina and its vasculature. *Anatomy & Cell Biology*, *45*, 38–46.

Li, H., Collado, M., Villasante, A., Strati, K., Ortega, S., Cañamero, M., ... Serrano, M. (2009). The Ink4/Arf locus is a barrier for iPS cell reprogramming. *Nature*, *460*, 1136–1139.

Li, X., Ma, W., Zhuo, Y., Yan, R.-T., & Wang, S.-D. (2010). Using neurogenin to reprogram chick RPE to produce photoreceptor-like neurons. *Investigative Ophthalmology & Visual Science*, *51*, 516–525.

Luz-Madrigal, A., Grajales-Esquivel, E., Mccorkle, A., Dilorenzo, A. M., Barbosa-Sabanero, K., ... Del Rio-Tsonis, K. (2014). Reprogramming of the chick retinal pigmented epithelium after retinal injury. *BMC Biology*, *12*, 28.

Ma, W., Yan, R. T., Li, X., & Wang, S. Z. (2009). Reprogramming retinal pigment epithelium to differentiate toward retinal neurons with Sox2. *Stem Cells*, *27*, 1376–1387.

MacLaren, R., & Pearson, R. (2007). Stem cell therapy and the retina. *Eye*, *21*, 1352–1359.

Maguire, A. M., High, K. A., Auricchio, A., Wright, J. F., Pierce, E. A., Testa, F., ... Rossi, S. (2009). Age-dependent effects of RPE65 gene therapy for Leber's congenital amaurosis: A phase 1 dose-escalation trial. *The Lancet*, *374*, 1597–1605.

Matsushima, D., Heavner, W., & Pevny, L. H. (2011). Combinatorial regulation of optic cup progenitor cell fate by SOX2 and PAX6. *Development*, *138*, 443–454.

Miao, C. H., Snyder, R. O., Schowalter, D. B., Patijn, G. A., Donahue, B., Winther, B., & Kay, M. A. (1998). The kinetics of rAAV integration in the liver. *Nature Genetics*, *19*, 13–15.

Narita, M., Nuñez, S., Heard, E., Narita, M., Lin, A. W., Hearn, S. A., ... Lowe, S. W. (2003). Rb-mediated heterochromatin formation and silencing of E2F target genes during cellular senescence. *Cell*, *113*, 703–716.

Philips, G. T., Stair, C. N., Lee, H. Y., Wroblewski, E., Berberoglu, M. A., Brown, N. L., & Mastick, G. S. (2005). Precocious retinal neurons: Pax6 controls timing of differentiation and determination of cell type. *Developmental Biology*, *279*, 308–321.

Qiu, G., Seiler, M. J., Thomas, B. B., Wu, K., Radosevich, M., & Sadda, S. R. (2007). Revisiting nestin expression in retinal progenitor cells in vitro and after transplantation in vivo. *Experimental Eye Research*, *84*, 1047–1059.

Raisler, B. J., Deng, W. T., Berns, K. I., & Hauswirth, W. W. (2005). Adeno-associated virus mediated gene therapy for vascular retinopathies. *Laboratory Techniques in Biochemistry and Molecular Biology*, *31*, 103–123.

Saini, J. S., Temple, S., & Stern, J. H. (2016). *Human retinal pigment epithelium stem cell (RPESC). Retinal degenerative diseases*. Mechanisms and Experimental Therapy. Cham: Springer International Publishing. pp. 557–562.

Salero, E., Blenkinsop, T. A., Corneo, B., Harris, A., Rabin, D., Stern, J. H., & Temple, S. (2012). Adult human RPE can be activated into a multipotent stem cell that produces mesenchymal derivatives. *Cell Stem Cell*, *10*, 88–95.

Sarkar, A., & Hochedlinger, K. (2013). The Sox family of transcription factors: Versatile regulators of stem and progenitor cell fate. *Cell Stem Cell*, *12*, 15–30.

Schmittgen, T. D., & Livak, K. J. (2008). Analyzing real-time PCR data by the comparative CT method. *Nature Protocols*, *3*, 1101–1108.

Shih, A. H., & Holland, E. C. (2006). Notch signaling enhances nestin expression in gliomas. *Neoplasia*, *8*, 1072-IN1.

Shin, D. H., Kwon, B. S., Chang, Y. P., Bae, S.-R., Kim, J., & Kim, J. W. (2003). Ultramicroscopical immunolocalization of PAX6 in the adult chicken retina. *Acta Histochemica*, *105*, 267–272.

Somers, A., Jean, J. C., Sommer, C. A., Omari, A., Ford, C. C., Mills, J. A., ... Smith, B. W. (2010). Generation of transgene-free lung disease-specific human induced pluripotent stem cells using a single excisable lentiviral stem cell cassette. *Stem Cells*, *28*, 1728–1740.

Tanaka, S., Kamachi, Y., Tanouchi, A., Hamada, H., Jing, N., & Kondoh, H. (2004). Interplay of SOX and POU factors in regulation of the Nestin gene in neural primordial cells. *Molecular and Cellular Biology*, *24*, 8834–8846.

Taranova, O. V., Magness, S. T., Fagan, B. M., Wu, Y., Surzenko, N., Hutton, S. R., & Pevny, L. H. (2006). SOX2 is a dose-dependent regulator of retinal neural progenitor competence. *Genes & Development*, *20*, 1187–1202.

Thomas, C. E., Storm, T. A., Huang, Z., & Kay, M. A. (2004). Rapid uncoating of vector genomes is the key to efficient liver transduction with pseudotyped adeno-associated virus vectors. *Journal of Virology*, *78*, 3110–3122.

Wang, B., Miyagoe-Suzuki, Y., Erica, Y., Ito, N., Nishiyama, T., Nakamura, M., ... Masuda, S. (2011). Reprogramming efficiency and quality of induced pluripotent stem cells (iPSCs) generated from muscle-derived fibroblasts of mdx mice at different ages. *PLOS Currents Muscular Dystrophy*, *3*, RRN1274.

Wang, S.-Z., Ma, W., Yan, R.-T., & Mao, W. (2010). Generating retinal neurons by reprogramming retinal pigment epithelial cells. *Expert Opinion on Biological Therapy*, *10*, 1227–1239.

Wiese, C., Rolletschek, A., Kania, G., Blyszczuk, P., Tarasov, K. V., Tarasova, Y., ... Wobus, A. M. (2004). Nestin expression—A property of multi-lineage progenitor cells? *Cellular and Molecular Life Sciences*, *61*, 2510–2522.

Yan, R.-T., Li, X., & Wang, S.-Z. (2013). Photoreceptor-like cells in transgenic mouse eyephotoreceptor generation in the mammalian eye. *Investigative Ophthalmology & Visual Science*, *54*, 4766–4775.

Yan, R. T., Liang, L., Ma, W., Li, X., Xie, W., & Wang, S. Z. (2010). Neurogenin1 effectively reprograms cultured chick retinal pigment epithelial cells to differentiate toward photoreceptors. *Journal of Comparative Neurology*, *518*, 526–546.

How to cite this article: Ezati R, Etemadzadeh A, Soheili Z-S, et al. The influence of rAAV2-mediated SOX2 delivery into neonatal and adult human RPE cells; a comparative study. *J Cell Physiol*. 2017;9999:1–14. https://doi.org/10.1002/jcp.25991